NASA Technical Memorandum 89042

Computational Analysis and Preliminary Redesign of the Nozzle Contour of the Langley Hypersonic CF_4 Tunnel

R. A. Thompson and Kenneth Sutton

MARCH 1987

NASA

NASA Technical Memorandum 89042

Computational Analysis and Preliminary Redesign of the Nozzle Contour of the Langley Hypersonic CF_4 Tunnel

R. A. Thompson and Kenneth Sutton
Langley Research Center
Hampton, Virginia

National Aeronautics
and Space Administration

Scientific and Technical
Information Branch

1987

Summary

A computational analysis, modification, and preliminary redesign study was performed on the nozzle contour of the Langley Hypersonic CF_4 Tunnel. Objectives of this work were, first, to study the origination and propagation of centerline disturbances measured at the exit and downstream of the exit in the existing nozzle; second, to determine the feasibility of modifying the present nozzle contour to eliminate the centerline disturbances; and, last, to redesign a nozzle contour for the CF_4 Tunnel for different reservoir and exit conditions using the original design methodology.

This study showed that the present nozzle of the CF_4 Tunnel was contoured incorrectly for the design reservoir and exit conditions and, in general, the diameter of the current nozzle was found to be too large over the length of the tunnel. The formation of disturbances, which are focused on the nozzle centerline, was predicted in terms of pitot pressure for the nominal and near-nominal reservoir conditions, and the predicted disturbance pattern across the nozzle exit was in agreement with measurements. A modified contour for the nozzle of the CF_4 Tunnel was designed for the portion downstream of the maximum turning angle. This new contour theoretically provided a uniform exit flow for the nominal reservoir condition. Attempts to modify the current nozzle contour in the throat region to produce uniform exit flow for the nominal reservoir condition were unsuccessful. Discussion of that modification effort is included for reference. New nozzle contours were designed for the CF_4 Tunnel to provide uniform flow at the nozzle exit with a Mach number and Reynolds number combination which closely matches that attainable in the Langley 20-Inch Mach 6 Tunnel. Two nozzle contours were designed: one having the same exit radius but a larger mass flow rate than that of the existing CF_4 Tunnel, and the other having the same mass flow rate but a smaller exit radius than that of the existing CF_4 Tunnel.

Introduction

The subject of the present report originates from the calibration results of the Langley Hypersonic CF_4 Tunnel reported by Midden and Miller (refs. 1 and 2). Of primary interest in this calibration are the centerline disturbances that were measured in the test section for most reservoir pressures and temperatures. Pitot pressure and total temperature surveys revealed that the flow at the nozzle exit was uniform only for reservoir temperatures greater than 1460°R with only a slight sensitivity to changes in stagnation pressure between roughly 1500 and 2500 psi. From those measurements, the best flow condition was found at the maximum stagnation temperature and pressure, which is $T_{t,1} \geq 1460°\text{R}$ and $p_{t,1} = 2500$ psi, respectively. The appearance of centerline disturbances was generally observed at lower reservoir temperatures. However, lowering the reservoir temperature has become a necessity for the routine operation of the CF_4 Tunnel since flow contamination became a serious problem when the tunnel was operated at high temperatures. This contamination posed a threat to the accuracy of test results, particularly heat-transfer studies, and to model surface instrumentation such as thin film gauges. To minimize these risks, the nominal operating temperature was lowered. As a result, the centerline disturbances are a constraint that must be considered when testing in the CF_4 Tunnel. At present, the only way to avoid this problem is to position the model in the inviscid test flow between the centerline disturbance and the nozzle boundary layer. In this region, the test-section flow has been shown to be uniform (ref. 2) and free from serious disturbances; however, the diameter of the available test core in the CF_4 Tunnel is now reduced by at least one-half. Consequently, the physical size of models tested in the tunnel is severely restricted and particular attention must be paid to the model orientation (angle of attack and yaw) within the reduced core of uniform flow.

In the present study, the problems and limitations of the current CF_4 Tunnel have been addressed from the standpoint of hypersonic nozzle design. Three objectives were undertaken in this study and are presented in this report. First, an analysis of the existing CF_4 Tunnel nozzle was performed to verify the original nozzle design and to determine the origination and propagation of the measured disturbances. The second objective was to determine if minor modifications to the existing nozzle contour would provide uniform flow at the nozzle exit for the design or for any new operating condition. Last, a preliminary design effort was undertaken to produce an entirely new nozzle contour for the CF_4 Tunnel for new reservoir and exit conditions. For this last objective, the major design parameters such as maximum turning angle and prescribed centerline Mach number distribution were unchanged from those used to design the existing CF_4 nozzle. The reasons for not modifying those parameters were twofold. First, the overall dimensions (i.e., nozzle length and exit diameter) were to remain similar to the existing nozzle. Second, rather than undertake a complete parametric study, the primary goal was to make a review exercise of the design procedure. As such, the nozzle designs presented in

this paper are preliminary and several items deserve further study.

Symbols

A, B	constants in wall temperature equation (see eq. (1))
C_1, C_2, C_3	virial coefficients
H	enthalpy, Btu/lbm
M	Mach number
$\dot{m}$	one-dimensional mass flow rate through nozzle throat, lbm/sec
N_{Re}	Reynolds number, ft^{-1}
p	pressure, psi
R	gas constant for CF_4, 565.2 $\mathrm{ft}^2/\mathrm{sec}^2/^\circ\mathrm{R}$
r	nozzle radius, in.
T	temperature, °R
T_r	gas temperature at nozzle throat, °R
u	velocity, ft/sec
u_ℓ	limiting velocity, $\sqrt{2H_{t,1}}$, ft/sec
x	axial distance, in.
z	compressibility factor
γ	ratio of specific heats
δ	boundary-layer thickness, in.
δ^*	boundary-layer displacement thickness, in.
ρ	density, $\mathrm{slug}/\mathrm{ft}^3$

Subscripts:

e	nozzle exit
ref	reference condition
$t, 1$	reservoir stagnation condition
$t, 2$	stagnation condition behind normal shock
w	nozzle wall
2	static condition at nozzle exit

Superscript:

$*$	condition at nozzle throat

Abbreviations:

BL	boundary layer
℄	nozzle centerline
MOC	method of characteristics

Computational Methods

The present numerical designs were performed using the computer codes of references 3 and 4 that solve the inviscid, irrotational flow equations by the method of characteristics (MOC). The designs were corrected by using boundary-layer solutions along the nozzle wall to account for viscous displacement effects. MOC and coupled boundary-layer solutions were also used to analyze the flow field in the existing CF_4 Tunnel nozzle. This approach is useful for the numerical analysis of internal flow problems but can be inadequate in some cases. The following sections describe the computational methods employed in this study in more detail.

Design Method of Characteristics

The design method of characteristics program was originally developed by Johnson et al. (ref. 3) and was later modified (ref. 4) to improve the numerical procedure and to add some additional capabilities. It was shown (ref. 4) that the modified solution procedure eliminated a small inflection in the nozzle contour in the area of maximum turning that had been present in earlier solutions. It was also shown that the modifications had a minimal effect on nozzle shape (less than a 2-percent change in nozzle radii downstream of maximum turning angle) so that the two codes produced nearly identical nozzle contours for the same set of design parameters. The inviscid contour of the existing CF_4 nozzle was designed with the earlier MOC program (i.e., ref. 3); but in the present study, the latest version (ref. 4) was used.

Johnson's program (ref. 4) is applicable to the inviscid design of both axisymmetric and two-dimensional supersonic nozzle contours and includes the capability of treating thermally and calorically imperfect gases in thermodynamic equilibrium. Design parameters available to the user include the reservoir conditions, the maximum turning angle of the nozzle, the centerline Mach number distribution in the initial expansion region, and the exit Mach number. For an imperfect-gas calculation, tabulated values of density ratio $(\rho/\rho_{t,1})$ and limiting velocity ratio (u/u_ℓ) as functions of Mach number are required for an isentropic expansion beginning at the design reservoir condition. In the design procedure, a Mach number distribution is first established along the nozzle centerline from the throat to

the desired exit Mach number. The final Mach line is constructed at this point, and then the program proceeds ("begins marching") backward toward the nozzle throat, solving the inviscid irrotational flow equations along left-running characteristics. The final inviscid contour is obtained by equating the mass flow through the nozzle along each computed characteristic.

A further discussion of the design procedure is warranted here since the design parameters chosen by the user can have a significant impact on the overall design. Figure 1(a) shows a diagram outlining the various regions used in the present design process for a supersonic nozzle. Region I is considered to be the throat region, region II is an area of radial or source flow, region III is a simple flow region where expansion waves that strike the wall are cancelled, and the last, region IV, is one of uniform flow. The line DE is the final Mach line with the Mach number at point D equal to the design exit Mach number. Point C is the inflection point in the nozzle contour and thus is the location of the maximum turning angle. In this design method, region II is approximated by source flow, and so the centerline Mach number distribution between points B and D can be determined by solving the radial flow equations. The Mach number distribution from A to B can then be prescribed between the value computed at point B and Mach 1 at point A.

Three options exist in Johnson's program (ref. 4) for describing the Mach number variation along line AB. First, a linear distribution can be used that results in a finite axial Mach number gradient at the throat (point A) and a relatively short throat section. The second option fits a third-order polynomial for the Mach number between A and B with a zero gradient constraint on Mach number at point A. A third available distribution uses a second-order polynomial for the Mach number variation and results in a finite, but controlled, axial gradient at the throat and also the shortest throat section of the three options.

Once the Mach number distribution is prescribed from A to B and computed from B to D, the only remaining initial data to be defined are along the final Mach line DE. These data are determined easily since the properties along DE are constant and are equal to the exit conditions. With this, the initial value problem is completely defined and may be solved in a marching manner. As described before, the program starts at line DE and proceeds backward toward the nozzle throat, computing each left-running characteristic from the centerline to the point where the stream function (i.e., the mass flow) is equal to the value at point C that was computed using the radial flow approximation. Once found, the point on each left-running characteristic then becomes a coordinate for the inviscid nozzle contour.

The two input parameters that have the most effect on the overall nozzle dimensions, for fixed reservoir and exit conditions, are the maximum turning angle and the centerline Mach number distribution in the initial expansion region (from points A to B). Both parameters can vary the expansion region and, therefore, the overall nozzle length in a substantial manner. Decreasing the maximum turning angle has the effect of lengthening the expansion region and vice versa. It is generally accepted that a smaller turning angle provides a better chance of obtaining uniform flow because of a more gradual expansion. In the existing CF_4 Tunnel, the nozzle was designed for a maximum turning angle of 16°, and this parameter was kept constant for the present calculations. With regard to the centerline Mach number distribution, the first of the options listed above (i.e., the linear variation) was used for the original CF_4 nozzle design and is also used in this report. Keeping these two parameters constant served the intended purposes of this paper. By not varying these values, a new nozzle could be designed with overall dimensions similar to those of the existing nozzle and, in doing so, the application of the design process could be easily demonstrated. A more detailed design study should include a careful examination of these parameters.

It is probably true that the third-order polynomial provides a better distribution of centerline Mach number since this fit matches the gradients at points A and B and provides a necessary condition for a straight sonic line at the throat; however, this Mach number variation results in a lengthy throat section. In addition to physical length constraints, the authors in reference 4 discuss other possible problems associated with a long and narrow expansion section. They point out that the heat loads associated with such a design may exceed normal structural limits and, therefore, need to be considered. That study also examined the effect of test gas on nozzle design and showed that a low gamma gas (that is, one having a low ratio of specific heats) such as tetrafluoromethane (CF_4) inherently produces a long and narrow expansion region and thus compounds the problems.

Analysis Method of Characteristics

In addition to design applications, the method of characteristics (MOC) can also be used for the analysis of supersonic internal flows for a given nozzle contour. For direct flow field calculations, the MOC requires different initial data from that for the design MOC and can involve difficulties associated with the formation of shock waves within the flow field.

In the present study, the basic analysis MOC code was taken from the text by Zucrow and Hoffman (ref. 5) and was modified for the CF_4 gas and existing nozzle shape. In this code, an initial line is computed at the throat by starting with the closed-form solution of Sauer (ref. 6) to obtain the sonic line. Sauer's method uses the transonic small perturbation equation and a power series solution to determine the equation of the sonic line in a converging-diverging throat. Since the sonic line is inappropriate to start the method of characteristics, an initial value line is computed where the radial perturbation velocity is zero. This initial data line extends from the wall at the nozzle minimum to a point on the centerline slightly downstream of the throat as shown in figure 1(b).

For the downstream solution, the flow field within the range of influence of the initial value line is computed first, and then the method "begins marching" toward the nozzle exit. In the marching procedure, a wall point is computed first by either extending a left-running characteristic until it intersects the fixed wall or by selecting points along the wall a priori and computing the intersecting left-running characteristics in an indirect fashion. After a wall point is computed, the solution proceeds along the right-running characteristic emanating from the wall until the nozzle centerline is reached. The solution continues downstream in this manner, computing from the wall to the nozzle centerline until the right-running characteristics cross the exit plane where they are terminated.

A difficulty in using the method of characteristics for analysis of a given nozzle shape is the possible formation of oblique shock waves within the flow field. Formation of an oblique shock is indicated by the crossing of two or more characteristics of the same family, and when this occurs, several options are available. First, the characteristics can be allowed to overlap and form a multivalued solution in the flow field. Alternatively, a characteristic can be terminated when crossing of the same family occurs. Another possibility is to fit an oblique shock wave within the flow field using shock jump relations. The most preferable way to handle crossing characteristics would be the latter option; however, the present formulation is not suited for this procedure because of the irrotational equations employed. Therefore, in the present analysis, the characteristics are allowed to overlap or they are terminated if the crossing prevents a complete solution.

Viscous Displacement Effects

The inviscid flow field computed by either method of characteristics described above must be coupled with viscous contributions near the nozzle wall to be accurate for design or analysis purposes. This requirement is true for the present hypersonic nozzle of interest since the boundary-layer growth is large over the relatively long nozzle. In earlier work, the integral boundary-layer method of reference 3 was modified by Hunt and Boney (appendix B of ref. 7) to account for the real-gas behavior of CF_4 gas due to vibration and high-pressure effects, and this method was employed to compute the viscous displacement effects. This code was coupled with the MOC program of reference 3 as part of the design procedure. In the present study, the integral boundary-layer code of reference 7 was only used to check the previous nozzle design. In the analysis of the existing nozzle and for the present design work, viscous displacement effects were computed using a finite-difference boundary-layer code developed by H. Harris Hamilton II of the Langley Research Center.

Boundary-layer edge conditions for the viscous calculations (x, r, M, u, p, and T) are obtained directly from the inviscid solution at the wall. At the solid surface, a steady-state wall temperature is computed with the analytic equation given by

$$T_w = \frac{T_r - A(r/r^*)^{1.8}}{1 + B(r/r^*)^{1.8}} \tag{1}$$

where T_r is the temperature of the gas at the nozzle throat. The constants A and B can be determined by defining the wall temperature at a point where r/r^* is large compared to unity and also at the nozzle exit. Equation (1) was presented in reference 3 in conjunction with the design of a hypersonic nitrogen tunnel. As noted in that study, this equation is expected to give a reasonable variation of wall temperature. For all calculations in this study, the boundary-layer and displacement thicknesses are assumed to be zero at the nozzle throat, and the viscous layer is assumed to be turbulent for the length of the nozzle. Turbulence is modeled in the finite-difference code by a two-layer eddy viscosity model (ref. 8) with instantaneous transition at the nozzle throat.

Implementing the viscous displacement effect on the design of a nozzle contour is usually done in a straightforward manner. In this study, a single pass with the boundary-layer code was made after the inviscid contour was computed and the conditions at the inviscid wall had been saved for input as the boundary-layer edge conditions. The computed displacement thicknesses were then added to the inviscid contour to generate the final nozzle coordinates. No smoothing of the inviscid or viscous contours was performed.

To correct the inviscid solution for the case where an analysis of a given nozzle shape is performed requires an iterative procedure. In this case, the process begins with an inviscid solution for the physical nozzle contour which, in actuality, already accounts for viscous displacement. In a manner similar to the design procedure, a boundary-layer solution is obtained along the nozzle wall using the inviscid solution to provide the edge conditions. The displacement thicknesses from the viscous solution are then subtracted from the original nozzle contour to provide a new "apparent wall." A second inviscid solution uses the apparent wall as the solid boundary and thus provides improved boundary-layer edge conditions. Next, a second boundary-layer solution is calculated along the original nozzle wall but using the new edge conditions. The resulting displacement thicknesses are again subtracted from the original nozzle contour to provide a better apparent wall. The iteration between inviscid and boundary-layer solutions as described above is continued until the displacement thicknesses (i.e., the apparent wall) are converged to within a plottable difference of approximately 3 percent. This process was generally found to require only two iterations for convergence in the present cases.

Thermodynamic and Transport Properties of CF_4 Gas

At high pressures, the CF_4 gas behaves in an imperfect manner, and relations for the thermodynamic and transport properties must account for this behavior. For present reservoir conditions, CF_4 remains undissociated as it is heated and expanded through the nozzle, but intermolecular force effects are significant in the reservoir and nozzle throat region where the pressures and densities are large. It is assumed in this study that the CF_4 gas remains in vibrational equilibrium (see appendix A in ref. 7) and that the flow in the inviscid region of the nozzle is isentropic. Consequently, the thermodynamic properties can be tabulated for values of Mach number by performing a one-dimensional expansion from the reservoir conditions to specified values of temperature. The computer code used to perform the isentropic expansion is based on the expressions and thermodynamic equations for CF_4 given by Hunt and Boney (ref. 9). This same code is currently used to determine test-section flow conditions in the CF_4 Tunnel (ref. 2). Its use is beneficial in this study since comparisons between calculated flow conditions and the present analysis will be on a consistent basis.

The finite-difference boundary-layer code of Hamilton uses the analytic expressions developed by Sutton (ref. 10) for the thermodynamic and transport properties of CF_4. These equations are simpler to apply and require less computer time than the full equations of reference 9. They are accurate to within ± 5 percent for thermal conductivity and specific heat and to less than ± 1 percent for the other properties.

The thermally perfect equation of state used in reference 10 was modified for this study to account for high-pressure effects encountered in the throat region. The equation of state developed for this study has the form

$$p = z\rho RT \tag{2}$$

where

$$z = 1.0 + C_1\bar{\rho} + C_2\bar{\rho}^2 + C_3\bar{\rho}^3$$

with

$$C_1 = 0.5238 - 428.4/T - 37920.0/T^2 - 1.720 \times 10^7/T^3 \qquad (\text{ft}^3/\text{slug})$$

$$C_2 = 0.02465 + 152.9/T - 1.044 \times 10^5/T^2 + 4.034 \times 10^7/T^3 \qquad (\text{ft}^6/\text{slug}^2)$$

$$C_3 = 7.086 \times 10^{-5}T - 0.03474 \qquad (\text{ft}^9/\text{slug}^3)$$

and

$$\bar{\rho} = p/RT$$

The full expressions given in reference 9 were also incorporated into the finite-difference boundary-layer program to check the validity of using the approximate relations. Comparisons of boundary-layer solutions using both methods to obtain thermodynamic and transport properties showed differences of less than ± 3 percent in displacement thicknesses. As a result, the approximate relations were considered adequate for use in the present boundary-layer calculations.

Results and Discussion

The objectives of the current study, as stated in the "Introduction," were as follows: (1) To analyze the existing CF_4 nozzle, (2) to determine if the existing nozzle could be modified to provide uniform test-section flow for nominal reservoir conditions, and (3) to redesign a new nozzle contour for different reservoir and exit conditions. Results for each objective are discussed in detail in the following subsections.

Analysis of Existing CF_4 Nozzle

Radially uniform test-section flow is obtained in the CF_4 Tunnel only when the reservoir temperature is equal to or greater than 1460°R. As discussed in reference 2, the contamination level in the flow increases with increasing temperature. Therefore, to

protect the tunnel and models and to provide a wider Reynolds number range, it is desirable to operate at lower stagnation temperatures. However, at lower $T_{t,1}$, disturbances are created in the internal flow field and appear on the nozzle centerline. Midden and Miller (refs. 1 and 2) have measured the disturbances at the nozzle exit and downstream of the exit. In some cases, the disturbance is characterized by a "spike" in the total pressure profiles measured across the nozzle exit, whereas other slightly different conditions have made the disturbance appear as a "dip" in total pressure at the centerline. The dip or spike character at the nozzle exit depends on the reservoir conditions, but it can alternate with axial distance downstream of the nozzle exit for a fixed reservoir condition. The local dip or spike in total pressure at the nozzle centerline has been measured to be generally 15 percent lower or higher, respectively, than the average pressure across the test section. This variation has been shown (ref. 2) to produce erroneous measurements of heating rates, surface pressures, and bow-shock shapes.

The existing CF_4 Tunnel nozzle was designed using the MOC program developed by Johnson et al. (ref. 3) and the modified boundary-layer code presented in reference 7. Since the revised version of this MOC code (ref. 4) was the primary design tool used in the present study, it was desirable to reproduce the existing nozzle contour as a check on the code and the existing nozzle. Calculations showed that from using the MOC code of reference 4 and the integral boundary-layer program described in reference 7, the existing contour could be reproduced for a reservoir condition of 2500 psi and 1260°R, an exit Mach number of 6, and a maximum turning angle of 16°.

There has been some question in the past about the design reservoir condition for the existing CF_4 Tunnel since it was not documented. It was generally assumed that the design condition was at 2500 psi and 1460°R since this was where the flow was most uniform. However, based on the present calculations, it appears that the actual design was performed for $p_{t,1} = 2500$ psi, but with $T_{t,1} = 1260$°R. The question arises as to why the measured disturbances occur at the lower stagnation temperature but disappear at the higher, presumably off-design, reservoir temperature. To answer this, a detailed review of the design method of characteristics (ref. 4) and the integral boundary-layer code, as modified in reference 7, was performed.

This review uncovered a subtle but significant error that was made in mating the inviscid and boundary-layer codes in the design process. The error arose from a mismatch of the reference enthalpies used for thermodynamic properties. In the integral boundary-layer code, the equation used for static enthalpy across the layer was based on a reference enthalpy of $H_{\text{ref}} = 0$ at $T_{\text{ref}} = 0$°R. However, the total enthalpy at the boundary-layer edge, which was input, was based on the equations given in reference 9 that have a reference enthalpy of $H_{\text{ref}} = 200$ Btu/lbm at a reference temperature T_{ref} of 820°R. The inconsistent use of enthalpy between the layer and edge directly affected the calculation of density in the boundary layer and thus affected the integration for displacement thickness in the integral approach.

Correction of the enthalpy mismatch was made to the integral boundary-layer code in the present study, and subsequent calculations showed the predicted boundary-layer and displacement thicknesses at the nozzle exit to be as much as 40 percent less than had previously been computed. Thus, contours designed for the CF_4 gas with the MOC and integral boundary-layer codes before this correction were generally too large in diameter, and this mismatch is apparently the major problem in the existing nozzle. Figure 2 shows a comparison of the existing nozzle contour with a new contour designed with the same MOC code but with the finite-difference boundary-layer program for the same design conditions ($p_{t,1} = 2500$ psi and $T_{t,1} = 1260$°R with $M_2 = 6$ exit flow). For this new contour, the enthalpy was based on a consistent reference in the inviscid and viscous programs. As shown, the existing nozzle radius is less than that predicted in the initial expansion region and eventually becomes larger than that predicted so that there is a large discrepancy in radius at the exit. The existing CF_4 nozzle is slightly longer than the newly designed contour as shown in figure 2. This difference is due to a cylindrical section, approximately 11 in. long, that was added to the original nozzle design.

A simple illustration of the problem presently existing in the CF_4 Tunnel can be made by considering the one-dimensional compressible flow theory assumed applicable for the inviscid flow at the nozzle exit. Figure 3 shows the nozzle-exit radius nondimensionalized by the throat radius as a function of Mach number according to the one-dimensional theory for various stagnation pressures and temperatures. These curves were obtained from the thermodynamic properties computed from an isentropic expansion using the equations of Hunt and Boney (ref. 9) and show the extreme sensitivity of Mach number to r/r^* for the CF_4 gas. For a design Mach number of 6 with $p_{t,1} = 2500$ psi and $T_{t,1} = 1260$°R, the inviscid radius ratio would be 38.25 according to this figure. This value can be compared with the

ratio for the existing nozzle, which is 44.85 as shown in the figure. This difference between inviscid radius and the existing radius would have to be made up by the boundary layer and, based on measurements (refs. 1 and 2), a boundary-layer thickness of this size at the nozzle exit is unrealistically large for the CF_4 nozzle. Figure 3 also shows that at $M_2 = 6$ the reservoir conditions of $T_{t,1} = 1460°R$ and $p_{t,1} = 2500$ psi could not be correct for the existing CF_4 Tunnel since there is no radial distance left to account for viscous displacement.

Some understanding of the centerline disturbances that exist in the CF_4 Tunnel was gained by finding that the existing nozzle was not contoured correctly for the design reservoir and exit conditions. Those calculations, however, did not establish the origination of the measured disturbances, nor did they provide any insight into the possible contour modifications that may be made. For these reasons, the analysis MOC code was used to obtain flow field solutions in the nozzle for several reservoir conditions. The conditions chosen correspond to instances where the nozzle-exit flow was uniform and also to the conditions where a spike and a dip occurred in the total pressure profile. Reservoir conditions for these three cases were as follows, respectively: $p_{t,1} = 2552$ psi and $T_{t,1} = 1481.4°R$; $p_{t,1} = 1742$ psi and $T_{t,1} = 1274.3°R$; and $p_{t,1} = 1515$ psi and $T_{t,1} = 1218.9°R$.

Wall temperature distributions along the nozzle were computed with equation (1) for use in the viscous part of the solutions. Since the actual CF_4 nozzle is heated by resistance heaters in the throat section to approximately the reservoir temperature before each run, the input wall temperature distributions were made to fit this variation. This process was accomplished by setting T_r equal to the reservoir temperature in equation (1). The wall temperatures at two axial stations were estimated from unpublished measurements made on the exterior nozzle wall during several tunnel runs by Raymond E. Midden of the Langley Research Center for use in the equation. Specifically, the wall temperature at the axial station where $r/r^* = 20$ was set to 660°R for reservoir temperatures around 1260°R and was set to 760°R for reservoir temperatures closer to 1460°R. The wall temperature at the nozzle exit was set to 530°R in all cases. Figure 4 shows the three input wall temperature distributions for the present cases. Note that each distribution begins at the respective reservoir temperature, remains constant for about 6 in., decreases rapidly to the value defined at the first station, and then approaches the temperature defined at the end of the nozzle. Also shown in this figure are the measured, exterior, nozzle wall temperatures for tunnel conditions similar to the present, low reservoir temperature cases. The assumed variation of wall temperature is in agreement with the general trend of the experimental measurements.

Numerical calculations for the three cases were performed with the analysis MOC and finite-difference boundary-layer codes described previously. Two complete iterations were performed between the MOC and boundary-layer solutions for each case. Results from these calculations are shown in figures 5 and 6. In figure 5(a), a representative computational mesh from a MOC solution is illustrated for one case, whereas figure 5(b) shows the corresponding contour plot of Mach number. Figure 6 compares the predicted and measured total pressure ratio profiles across the test section at the nozzle exit for each case.

The computational mesh in figure 5(a) shows the actual left- and right-running characteristics computed as part of the MOC solution for the case where a spike in total pressure was measured at the nozzle exit. As can be seen, the mesh used was fairly coarse, especially in the downstream portion of the nozzle. The indirect method of computing the intersection of left-running characteristics with the predefined wall was used for these calculations so that some control over spacing could be achieved. Arbitrary refinement of the grid was not possible, however, because of the crossing of characteristics predicted in the flow field near the nozzle exit. By using a coarser grid, the number of crossing characteristics was limited and complete solutions were obtainable. Crossing of right-running characteristics generally occurred near the nozzle centerline and the nozzle exit for the three cases considered and indicated the formation of oblique shock waves within the nozzle. Note in figure 5(a) that the characteristic mesh is well-behaved in the throat and initial expansion region until $x = 35$ in. After the 35-in. station, the right-running characteristics alternately compress and expand for the remainder of the nozzle length.

Figure 5(b) shows the Mach contour for the same case where a spike in total pressure exists and clearly illustrates the disturbances in the flow field. In this and in the other cases, disturbances were found to emanate all along the nozzle wall downstream of $x = 35$ in. For this case in particular, there appears to be strong compressions or shock waves that strike the centerline between 65 in. and the nozzle exit ($x = 93$ in.). By tracing these disturbances backward with the aid of figure 5(a), it is observed that these waves originate from the nozzle wall between 35 and 45 in. The occurrence of these waves was noted for each case; however, the exact location and

the strength of the waves varied with the reservoir condition. In the first case, where the most uniform exit flow was measured, a weak compression wave was found to intersect the centerline at around 65 in. where it was reflected back toward the wall. For the second case (shown in fig. 5), where a spike in total pressure occurred, two strong waves are seen coming from the nozzle wall and intersecting the centerline. The first is reflected at 65 in. and the second intersects the centerline almost exactly at the nozzle exit. Note in figure 5(b) that the reflection of the first wave from the centerline intersects with a second wave coming from the wall to produce a rather complex flow. In the last case, where a dip in total pressure was measured, two strong waves were again found to emanate from the wall and intersect the centerline. This time, however, the second wave hit the centerline about 10 in. upstream of the nozzle exit.

The location of the compression or shock waves can be correlated with the measured centerline disturbances. In figure 6, the ratio of total pressures at the nozzle exit to the reservoir pressure is plotted across the test section from the centerline to the nozzle wall. Both measured and predicted values are included for comparison. In addition, experimental and predicted free-stream values of Mach number, static pressure, and temperature are compared. Note also that the predicted displacement and boundary-layer thicknesses at the nozzle exit are marked at the appropriate radius on the figure.

In figure 6(a), the total pressure profile is shown for the condition where the most uniform flow was measured. The experimental data in this case show a slight saddlelike distribution and a small rise in pressure on the centerline, but the data are fairly uniform across the test section. The inviscid pressure predictions from the analysis MOC code are in good agreement with experiment for a radius between 3 and 8 in. Closer to the centerline ($r < 3$ in.), the agreement between prediction and experiment is not as good, and the computed solution shows a slightly larger rise in pressure on the centerline.

In the second case, a spike in pressure was measured on the nozzle centerline as shown in figure 6(b). Prediction and experiment are again in good agreement between 3 and 8 in. from the centerline, whereas the computation tends to overpredict the pressure closer to the centerline. However, the spike behavior of the measured data on the centerline is also exhibited in the calculation. Experimental data for the last case were obtained from Midden and showed similar results (fig. 6(c)). Namely, experiment and theory agree quite well across the test section except within 3 in. from the centerline. The general behavior of the centerline disturbance is captured, however, and a dip in total pressure is predicted.

The poorer quantitative agreement between experiment and prediction in the innermost core of the test section ($r < 3$ in.) for these cases is not too surprising since indications are that shock waves are formed and reflected in this region and a complex flow field evolves. In these areas, the present method of analysis cannot be expected to be accurate; however, the solutions do show good qualitative agreement. In correlating the flow field predictions with the measured disturbances, it appears that the spike in total pressure is caused by a strong compression (or shock) wave that intersects the centerline just upstream of the nozzle exit. For the case of a dip in pressure, the flow field solution indicates that a compression wave intersects the centerline well upstream of the exit and is followed by an expansion region that crosses the exit plane, thereby causing the local minimum in total pressure. The alternating dip and spike character of the centerline flow downstream of the nozzle exit measured by Midden and Miller (refs. 1 and 2) could also be explained in this context. In the case of the most uniform exit flow, it appears that the compression waves formed from the turning contour are not as severe, and the strongest waves do not intersect the centerline in the proximity of the exit plane.

The detailed flow field analysis performed for the three representative cases revealed the origination of the measured disturbances in the CF_4 Tunnel. Most importantly, the analysis showed that the disturbances are not created in the upstream throat section of the nozzle but are instead formed from the nozzle wall downstream of the $x = 35$ in. station. All indications are that the flow expansion is too great initially because of the larger than necessary diameter of the contour for the near-nominal reservoir conditions. After excessive expansion, the flow is then turned nonisentropically through the remaining portion of the nozzle. At the higher reservoir temperature, the flow is not expanded too much judging by the maximum Mach number attained. Still, in this case the flow is not turned without creating some weak disturbances.

Modification of Existing Nozzle

A major objective of this study was to design a modification to the existing CF_4 Tunnel nozzle that would produce a uniform exit flow for reservoir conditions that were tolerable with regard to the contamination problem. If a simple contour modification could be devised, then the tunnel could realize its full capability, in terms of usable test-section flow, with minimum alteration. Since the existing

nozzle consists of four separate sections, it would be fairly easy to change the contour within a region by simply replacing the affected section. It was hoped further that a simple redesign of the throat section alone could be devised to produce the uniform flow since this is probably the least expensive modification. Unfortunately, these design objectives have not been fully met in this study; however, a discussion of the results of this effort may be useful and is included here.

Because of the nonisentropic turning of the flow in the current CF_4 nozzle for the nominal reservoir conditions, it is not clear whether any modification can be made to the throat-section contour that would also satisfy the downstream contour. An easier alternative, but less preferable from a cost standpoint, would involve keeping the throat section fixed and recontouring the nozzle downstream of the maximum turning location. This modification has been accomplished numerically in the present study using the following reservoir and exit conditions: $p_{t,1} = 1500$ psi, $T_{t,1} = 1260°$R, and $M_2 = 6$ exit flow.

The new contour was obtained by first performing a MOC calculation and coupled boundary-layer solution for the initial expansion region of the present nozzle that is to be kept fixed. Afterward, the remaining nozzle contour was designed using the initial data provided from the MOC solution. The results of this modification are shown in figure 7 where the existing CF_4 nozzle contour is compared with the new contour design. The new nozzle contour is identical to the existing one up to the maximum turning angle. Downstream of that point, the new contour has a smaller radius than the current nozzle and the differences increase over the remaining length. This modification is in accord with the earlier findings where the existing nozzle contour was established to be generally too large in diameter. Note in figure 7 that the newly contoured section comprises 90 percent of the overall length of the nozzle.

A promising method for modifying supersonic nozzle contours has recently been developed by Erlebacher et al. (ref. 11) at the Langley Research Center for use in modifying the Langley 8-Foot High-Temperature Tunnel. The basic assumption in their approach is that the flow through a correctly designed inviscid contour can be reversed since it is an isentropic process. With this approach, the modification procedure begins at the nozzle exit where an inviscid solution is obtained for the reversed flow going into the nozzle toward the throat. Initial conditions for this solution are provided by specifying a uniform flow at the nozzle exit (now the entrance). Boundary conditions are set by the physical nozzle wall. The backward flowing inviscid solution is obtained up to the last point on the nozzle wall that is to be unmodified. This inviscid solution then provides initial data to start a method of characteristics solution from the end of the unmodified nozzle wall toward the throat. Boundary data for that region are set by defining the remaining centerline Mach number distribution between the inviscid solution and the throat. With this definition and the initial data from the backward-flow solution, the method of characteristics can provide a new contour for the nozzle throat section. Viscous corrections are determined by sweeping forward in a normal manner with the new throat section and then repeating the backward-design process in an iterative manner.

In their work, Erlebacher et al. (ref. 11) used a full solution of the Euler equations for the backward-moving flow field and for the forward-sweeping calculations. In the present study, these same ideas have been applied in an attempt to modify the throat section of the CF_4 nozzle; however, the method of characteristics was employed to compute the backward-flow solution since the thermodynamics were already developed for the MOC code.

Several different stagnation and exit conditions were considered for the CF_4 nozzle, and inviscid solutions for the backward flow were obtained up to the location of maximum turning. At this location, however, problems arose that Erlebacher et al. (ref. 11) did not encounter. Examination of the backward-flow solution revealed the existence of crossing characteristics emanating from the unmodified wall section. In reference 11, the authors discussed the possible formation of shock waves in the backward-moving flow field. Their conclusion is that the design process can continue with the complete Euler solution, and if the waves are weak enough, they may disappear when the viscous corrections are added. In the present case, the shock waves that were formed in the backward-flow field by the CF_4 nozzle contour invalidate the MOC for use in the modification procedure. Continuing the modification process outlined in reference 11 will apparently demand using the full solution to the Euler equations. This process, which would require modification of the computer codes described in reference 11 to incorporate the imperfect-gas behavior of CF_4, has not been done in the present study.

Another approach to the modification of the CF_4 Tunnel that has not been tried, but may be useful, is to study the effects of arbitrarily changing the throat or downstream section contours. One could intuitively devise new contours and then perform flow field analyses like those done in this paper to examine the effects on the exit flow. With this approach, it would likely be very difficult to

arrive at the modifications necessary to produce a uniform flow, but such a parametric study might provide insight.

Design of New CF_4 Nozzle

The last objective in this study was to design a nozzle contour for the CF_4 Tunnel for reservoir and exit conditions different from those for which the nozzle was originally designed. Unlike the modification effort, this process entailed fewer constraints and was successful. The primary purpose of a new nozzle design is to match the conditions in the CF_4 Tunnel more closely to the free-stream conditions of other test facilities. Matching the free-stream Reynolds numbers and Mach numbers of the CF_4 Tunnel with those of another wind tunnel using air as the test gas is important since the effect of shock density ratio or gamma (γ) may be studied independent of Mach number or Reynolds number differences. At present, the Langley 20-Inch Mach 6 Tunnel is the most appropriate facility for this purpose, and thus the new design of the CF_4 nozzle was constrained to match the Reynolds number and Mach number of this facility. At the lowest reservoir pressure condition in the 20-Inch Mach 6 Tunnel, a test-section Mach number of 5.77 and a Reynolds number of 0.64×10^6 per foot are obtained (ref. 12). An isentropic expansion of the CF_4 gas from reservoir conditions of $p_{t,1} = 1600$ psi and $T_{t,1} = 1260°$R gives approximately the same Reynolds number for $M_2 = 5.77$. Therefore, for the present nozzle design, these values of reservoir and exit conditions were selected.

The nozzle design in this study was performed using the same inviscid technique used in the previous CF_4 Tunnel design. The maximum turning angle was kept fixed at 16°, and the centerline Mach number variation in the throat section was defined using the linear fit described previously so that the overall nozzle dimensions would remain similar. For the viscous corrections, the finite-difference boundary-layer program of Hamilton was used. The boundary layer was assumed turbulent for the length of the new nozzle contour, and the wall temperature variation was defined using equation (1) in the same manner discussed previously. In effect, all design variables except reservoir and exit conditions were the same as those used to design the existing nozzle. Proceeding in this manner allowed direct comparisons of new designs with the existing nozzle and was sufficient for the purposes of this study.

An additional constraint on the nozzle design for the CF_4 Tunnel involves the mass flow rate. Primarily for economic reasons (ref. 2), it is preferable to keep the same mass flow rate of the present tunnel in the new nozzle design. This requirement causes a slight dilemma as shown in figure 8. In this figure the inviscid core radius of the CF_4 nozzle exit is plotted as a function of the one-dimensional mass flow rate through the throat for the new reservoir and exit Mach number conditions. This figure shows that retaining the same mass flow rate as that of the existing tunnel operating at nominal reservoir conditions results in an inviscid core exit radius of about 6.4 in. This radius is less than the approximate 8-in. inviscid radius currently provided in the CF_4 Tunnel (assuming that there was no centerline disturbance). When the disturbance is taken into account by testing off the centerline, the existing inviscid radius then drops to about 4 in. and, thus, the present inviscid design offers some improvement. At the other extreme, retaining approximately the same inviscid radius as that of the current nozzle as designed (i.e., 8 in. by neglecting the centerline disturbance) requires a mass flow rate which is nearly 60 percent greater than that currently used. In the present study, new CF_4 nozzles have been designed for both conditions: the first has about the same mass flow rate as that of the current tunnel, and the second has approximately the same inviscid exit radius as that of the existing nozzle.

Figure 9 shows the nozzle-wall temperature distributions used for the present designs, and the new nozzle contours computed using the MOC and boundary-layer codes are shown in figure 10. A magnified view of the throat region is presented in figure 11. A listing of the wall coordinates for both designs is presented in table I. These tables were obtained by cubic spline interpolation of the computed coordinates so that even axial spacing of the tabulated values could be presented. The radial distance at the throat ($x = 0$) was obtained by extrapolating the predicted contour backwards since a MOC solution was not obtained at that point. This result occurred because the sonic point on the nozzle centerline is slightly downstream of the nozzle minimum. The reservoir and predicted exit properties for the new CF_4 nozzles are listed and compared with those from the 20-Inch Mach 6 Tunnel in the table on page 11.

Comparing the new nozzle contours with the existing CF_4 nozzle, which has a design error, showed substantial differences in both radius and length for the case where the mass flow rate is approximately equal. In that case, the throat radius is identical to the existing nozzle ($r^* = 0.2229$ in.), but the total length is reduced from the present 93 in. to 70.4 in., and the physical exit radius is 7.89 in. as compared with 10 in. The throat radius of the contour, which results in approximately the same inviscid exit radius, is only slightly greater ($r^* = 0.2792$ in.). The

overall length in that case was about 88 in., and the physical exit radius was computed to be 9.85 in. Note that the larger throat radius results in a longer and narrower initial expansion region as shown in figure 11.

Property	CF_4 Tunnel	20-Inch Mach 6 Tunnel[a]
$p_{t,1}$, psi	1600	31
$T_{t,1}$, °R	1260	866
p_2, psi	8.05×10^{-2}	2.49×10^{-2}
T_2, °R	386.5	113.1
M_2	5.77	5.77
$N_{Re,2}$, ft^{-1} . . .	5.76×10^5	6.38×10^5

[a]Data taken from reference 12.

The nozzle designs presented in this paper were performed on a preliminary basis and several items should be considered for further study. As discussed previously, no parametric study of maximum turning angle or initial Mach number distribution was made, and therefore these warrant examination. Since the numerical capability exists (ref. 11) to compute internal flow fields using the full Euler and Navier-Stokes equations, these calculations should obviously be considered for verification of any design. In addition, once a preliminary design contour is chosen, it would be possible to vary the reservoir conditions parametrically to study the effects of off-design conditions. Finally, no attempt has been made to design the settling chamber or the converging contour upstream of the throat section. The effects of those component designs can best be determined by solutions to the Euler and Navier-Stokes equations.

Concluding Remarks

An analysis, modification, and preliminary design study was performed for the nozzle contour of the Langley Hypersonic CF_4 Tunnel. Objectives of this work were, first, to study the origination and propagation of centerline disturbances measured in the existing tunnel; second, to determine the feasibility of modifying the present nozzle contour to eliminate the centerline disturbances; and, last, to redesign a nozzle contour for the CF_4 Tunnel for different reservoir and exit conditions using the original design methodology.

A review of the procedure used in the original design of the CF_4 Tunnel revealed that the present nozzle was contoured incorrectly for the design reservoir and exit conditions. In general, the diameter of the current nozzle was shown to be too large over the length of the tunnel. The formation of disturbances, which are focused on the nozzle centerline, was predicted for the nominal reservoir conditions, and the predicted disturbance pattern across the nozzle exit was in agreement with the measurements. A modified contour for the nozzle of the CF_4 Tunnel was designed for the portion downstream of the maximum turning angle. This new contour theoretically provided a uniform exit flow for the nominal reservoir condition. New nozzle contours were designed for the CF_4 Tunnel to provide uniform flow at the nozzle exit with a Mach number and Reynolds number combination which closely matches that attainable in the Langley 20-Inch Mach 6 Tunnel. Two nozzle contours were designed: one having the same exit radius but a larger mass flow rate than that of the existing CF_4 Tunnel, and the other having the same mass flow rate but a smaller exit radius than that of the existing CF_4 Tunnel.

NASA Langley Research Center
Hampton, VA 23665-5225
January 13, 1987

References

1. Midden, R. E.; and Miller, C. G.: *Description and Preliminary Calibration Results for the Langley Hypersonic CF_4 Tunnel.* NASA TM-78800, 1978.
2. Midden, Raymond E.; and Miller, Charles G., III: *Description and Calibration of the Langley Hypersonic CF_4 Tunnel—A Facility for Simulating Low γ Flow as Occurs for a Real Gas.* NASA TP-2384, 1985.
3. Johnson, Charles B.; Boney, Lillian R.; Ellison, James C.; and Erickson, Wayne D.: *Real-Gas Effects on Hypersonic Nozzle Contours With a Method of Calculation.* NASA TN D-1622, 1963.
4. Johnson, Charles B.; and Boney, Lillian R.: *A Method for Calculating a Real-Gas Two-Dimensional Nozzle Contour Including the Effects of Gamma.* NASA TM X-3243, 1975.
5. Zucrow, Maurice J.; and Hoffman, Joe D.: *Gas Dynamics—Volume II.* John Wiley & Sons, c.1977.
6. Sauer, R.: *General Characteristics of the Flow Through Nozzles at Near Critical Speeds.* NACA TM 1147, 1947.
7. Jones, Robert A.; and Hunt, James L. (appendix A by James L. Hunt, Kathryn A. Smith, and Robert B. Reynolds and appendix B by James L. Hunt and Lillian R. Boney): *Use of Tetrafluoromethane To Simulate Real-Gas Effects on the Hypersonic Aerodynamics of Blunt Vehicles.* NASA TR R-312, 1969.

8. Harris, Julius E.: *Numerical Solution of the Equations for Compressible Laminar, Transitional, and Turbulent Boundary Layers and Comparisons With Experimental Data.* NASA TR R-368, 1971.
9. Hunt, James L.; and Boney, Lillian R.: *Thermodynamic and Transport Properties of Gaseous Tetrafluoromethane in Chemical Equilibrium.* NASA TN D-7181, 1973.
10. Sutton, Kenneth: *Relations for the Thermodynamic and Transport Properties in the Testing Environment of the Langley Hypersonic CF_4 Tunnel.* NASA TM-83220, 1981.
11. Erlebacher, Gordon; Kumar, Ajay; Anderson, E. Clay; Rogers, R. Clayton; Dwoyer, Douglas L.; Salas, Manuel; and Harris, Julius E.: A Computational Design Procedure for Actively Cooled Hypersonic Wind-Tunnel Nozzles Subject to Wall Shape Constraints. Paper presented at the CFD in Aerospace Design Workshop (Tullahoma, Tennessee), Univ. of Tennessee Space Inst., June 4–6, 1985.
12. Miller, C. G.; and Smith, F. M.: Langley Hypersonic Facilities Complex—Description and Application. AIAA-86-0741, Mar. 1986.

Table I. Design Wall Coordinates for the CF_4 Nozzle

(a) $\dot{m}$ equal

x, in.	r, in.
0.000	0.2229
.200	.2240
.400	.2264
.600	.2299
.800	.2347
1.000	.2406
1.200	.2478
1.400	.2558
1.600	.2650
1.800	.2761
2.000	.2888
2.200	.3032
2.400	.3194
2.600	.3376
2.800	.3581
3.000	.3811
3.200	.4071
3.400	.4366
3.600	.4703
3.800	.5083
4.000	.5501
4.200	.5950
4.400	.6425
4.600	.6921
4.800	.7434
5.000	.7962
5.200	.8501
5.400	.9050
5.600	.9606
5.800	1.0169
6.000	1.0738
6.200	1.1311
6.400	1.1888
6.600	1.2468
6.800	1.3050
7.000	1.3635
7.200	1.4221
7.400	1.4808
7.600	1.5397
7.800	1.5987
8.000	1.6577
8.200	1.7168
8.400	1.7760
8.600	1.8353
8.800	1.8946
9.000	1.9539

x, in.	r, in.
9.200	2.0129
9.400	2.0716
9.600	2.1298
9.800	2.1875
10.000	2.2448
10.200	2.3015
10.400	2.3578
10.600	2.4136
10.800	2.4688
11.000	2.5236
11.200	2.5778
11.400	2.6316
11.600	2.6848
11.800	2.7376
12.000	2.7898
12.200	2.8416
12.400	2.8928
12.600	2.9436
12.800	2.9940
13.000	3.0438
13.200	3.0932
13.400	3.1420
13.600	3.1905
13.800	3.2384
14.000	3.2859
14.200	3.3329
14.400	3.3795
14.600	3.4257
14.800	3.4714
15.000	3.5167
15.200	3.5616
15.400	3.6060
15.600	3.6501
15.800	3.6937
16.000	3.7370
16.200	3.7798
16.400	3.8222
16.600	3.8643
16.800	3.9059
17.000	3.9472
17.200	3.9881
17.400	4.0286
17.600	4.0688
17.800	4.1086
18.000	4.1480
18.200	4.1871

Table I. Continued

(a) Continued

x, in.	r, in.
18.400	4.2258
18.600	4.2642
18.800	4.3023
19.000	4.3399
19.200	4.3772
19.400	4.4142
19.600	4.4508
19.800	4.4871
20.000	4.5231
20.200	4.5587
20.400	4.5940
20.600	4.6290
20.800	4.6637
21.000	4.6982
21.200	4.7322
21.400	4.7660
21.600	4.7995
21.800	4.8327
22.000	4.8656
22.200	4.8982
22.400	4.9305
22.600	4.9626
22.800	4.9944
23.000	5.0259
23.200	5.0571
23.400	5.0880
23.600	5.1186
23.800	5.1490
24.000	5.1790
24.200	5.2088
24.400	5.2384
24.600	5.2677
24.800	5.2968
25.000	5.3258
25.200	5.3546
25.400	5.3832
25.600	5.4117
25.800	5.4399
26.000	5.4679
26.200	5.4957
26.400	5.5233
26.600	5.5507
26.800	5.5778
27.000	5.6047
27.200	5.6313
27.400	5.6576

x, in.	r, in.
27.600	5.6837
27.800	5.7096
28.000	5.7352
28.200	5.7606
28.400	5.7857
28.600	5.8106
28.800	5.8353
29.000	5.8598
29.200	5.8840
29.400	5.9080
29.600	5.9317
29.800	5.9552
30.000	5.9784
30.500	6.0355
31.000	6.0915
31.500	6.1464
32.000	6.2000
32.500	6.2521
33.000	6.3029
33.500	6.3527
34.000	6.4016
34.500	6.4492
35.000	6.4955
35.500	6.5407
36.000	6.5851
36.500	6.6286
37.000	6.6709
37.500	6.7119
38.000	6.7519
38.500	6.7914
39.000	6.8300
39.500	6.8675
40.000	6.9037
40.500	6.9390
41.000	6.9736
41.500	7.0075
42.000	7.0407
42.500	7.0731
43.000	7.1044
43.500	7.1347
44.000	7.1641
44.500	7.1929
45.000	7.2211
45.500	7.2488
46.000	7.2758
46.500	7.3018

Table I. Continued

(a) Concluded

x, in.	r, in.
47.000	7.3267
47.500	7.3509
48.000	7.3744
48.500	7.3975
49.000	7.4200
49.500	7.4420
50.000	7.4633
50.500	7.4839
51.000	7.5039
51.500	7.5230
52.000	7.5413
52.500	7.5591
53.000	7.5764
53.500	7.5933
54.000	7.6096
54.500	7.6254
55.000	7.6408
55.500	7.6558
56.000	7.6701
56.500	7.6837
57.000	7.6966
57.500	7.7090
58.000	7.7209
58.500	7.7324

x, in.	r, in.
59.000	7.7436
59.500	7.7543
60.000	7.7646
60.500	7.7745
61.000	7.7840
61.500	7.7931
62.000	7.8018
62.500	7.8101
63.000	7.8181
63.500	7.8257
64.000	7.8329
64.500	7.8395
65.000	7.8457
65.500	7.8514
66.000	7.8568
66.500	7.8619
67.000	7.8668
67.500	7.8713
68.000	7.8755
68.500	7.8795
69.000	7.8832
69.500	7.8863
70.000	7.8889
70.425	7.8910

Table I. Continued

(b) r_e equal

x, in.	r, in.
0.000	0.2792
.200	.2802
.400	.2822
.600	.2851
.800	.2890
1.000	.2939
1.200	.2997
1.400	.3065
1.600	.3141
1.800	.3223
2.000	.3316
2.200	.3425
2.400	.3547
2.600	.3682
2.800	.3830
3.000	.3993
3.200	.4173
3.400	.4370
3.600	.4586
3.800	.4824
4.000	.5086
4.200	.5375
4.400	.5697
4.600	.6054
4.800	.6445
5.000	.6864
5.200	.7309
5.400	.7775
5.600	.8260
5.800	.8760
6.000	.9274
6.200	.9799
6.400	1.0334
6.600	1.0877
6.800	1.1427
7.000	1.1984
7.200	1.2545
7.400	1.3111
7.600	1.3682
7.800	1.4255
8.000	1.4831
8.200	1.5410
8.400	1.5991
8.600	1.6573
8.800	1.7158
9.000	1.7743

x, in.	r, in.
9.200	1.8330
9.400	1.8918
9.600	1.9506
9.800	2.0095
10.000	2.0685
10.200	2.1276
10.400	2.1866
10.600	2.2457
10.800	2.3048
11.000	2.3640
11.200	2.4233
11.400	2.4824
11.600	2.5413
11.800	2.5997
12.000	2.6579
12.200	2.7156
12.400	2.7730
12.600	2.8299
12.800	2.8865
13.000	2.9427
13.200	2.9985
13.400	3.0539
13.600	3.1089
13.800	3.1635
14.000	3.2178
14.200	3.2716
14.400	3.3250
14.600	3.3780
14.800	3.4305
15.000	3.4827
15.200	3.5345
15.400	3.5859
15.600	3.6369
15.800	3.6876
16.000	3.7378
16.200	3.7877
16.400	3.8372
16.600	3.8864
16.800	3.9351
17.000	3.9835
17.200	4.0315
17.400	4.0791
17.600	4.1264
17.800	4.1733
18.000	4.2198
18.200	4.2660

Table I. Continued

(b) Continued

x, in.	r, in.
18.400	4.3119
18.600	4.3575
18.800	4.4027
19.000	4.4475
19.200	4.4921
19.400	4.5363
19.600	4.5802
19.800	4.6237
20.000	4.6669
20.200	4.7098
20.400	4.7523
20.600	4.7946
20.800	4.8365
21.000	4.8781
21.200	4.9194
21.400	4.9604
21.600	5.0011
21.800	5.0415
22.000	5.0816
22.200	5.1214
22.400	5.1609
22.600	5.2002
22.800	5.2391
23.000	5.2778
23.200	5.3162
23.400	5.3543
23.600	5.3922
23.800	5.4297
24.000	5.4670
24.200	5.5040
24.400	5.5408
24.600	5.5773
24.800	5.6135
25.000	5.6494
25.200	5.6852
25.400	5.7206
25.600	5.7559
25.800	5.7908
26.000	5.8256
26.200	5.8601
26.400	5.8943
26.600	5.9283
26.800	5.9620
27.000	5.9955
27.200	6.0287
27.400	6.0617

x, in.	r, in.
27.600	6.0944
27.800	6.1269
28.000	6.1591
28.200	6.1912
28.400	6.2229
28.600	6.2545
28.800	6.2859
29.000	6.3170
29.200	6.3479
29.400	6.3786
29.600	6.4091
29.800	6.4394
30.000	6.4695
30.500	6.5438
31.000	6.6169
31.500	6.6889
32.000	6.7601
32.500	6.8303
33.000	6.8997
33.500	6.9680
34.000	7.0351
34.500	7.1007
35.000	7.1649
35.500	7.2278
36.000	7.2897
36.500	7.3506
37.000	7.4105
37.500	7.4690
38.000	7.5262
38.500	7.5824
39.000	7.6379
39.500	7.6925
40.000	7.7458
40.500	7.7979
41.000	7.8492
41.500	7.8996
42.000	7.9491
42.500	7.9978
43.000	8.0456
43.500	8.0922
44.000	8.1379
44.500	8.1829
45.000	8.2273
45.500	8.2709
46.000	8.3134
46.500	8.3550

Table I. Concluded

(b) Concluded

x, in.	r, in.
47.000	8.3956
47.500	8.4356
48.000	8.4751
48.500	8.5140
49.000	8.5521
49.500	8.5892
50.000	8.6253
50.500	8.6607
51.000	8.6955
51.500	8.7297
52.000	8.7634
52.500	8.7964
53.000	8.8288
53.500	8.8604
54.000	8.8913
54.500	8.9213
55.000	8.9506
55.500	8.9794
56.000	9.0077
56.500	9.0356
57.000	9.0630
57.500	9.0898
58.000	9.1158
58.500	9.1411
59.000	9.1657
59.500	9.1897
60.000	9.2132
60.500	9.2363
61.000	9.2589
61.500	9.2810
62.000	9.3027
62.500	9.3240
63.000	9.3448
63.500	9.3650
64.000	9.3844
64.500	9.4031
65.000	9.4214
65.500	9.4392
66.000	9.4567
66.500	9.4737
67.000	9.4903
67.500	9.5065

x, in.	r, in.
68.000	9.5224
68.500	9.5378
69.000	9.5528
69.500	9.5675
70.000	9.5818
70.500	9.5956
71.000	9.6087
71.500	9.6213
72.000	9.6334
72.500	9.6452
73.000	9.6568
73.500	9.6680
74.000	9.6788
74.500	9.6894
75.000	9.6995
75.500	9.7094
76.000	9.7190
76.500	9.7282
77.000	9.7371
77.500	9.7458
78.000	9.7541
78.500	9.7621
79.000	9.7698
79.500	9.7773
80.000	9.7844
80.500	9.7912
81.000	9.7973
81.500	9.8032
82.000	9.8087
82.500	9.8141
83.000	9.8192
83.500	9.8241
84.000	9.8287
84.500	9.8331
85.000	9.8373
85.500	9.8412
86.000	9.8448
86.500	9.8483
87.000	9.8516
87.500	9.8546
88.000	9.8570
88.219	9.8580

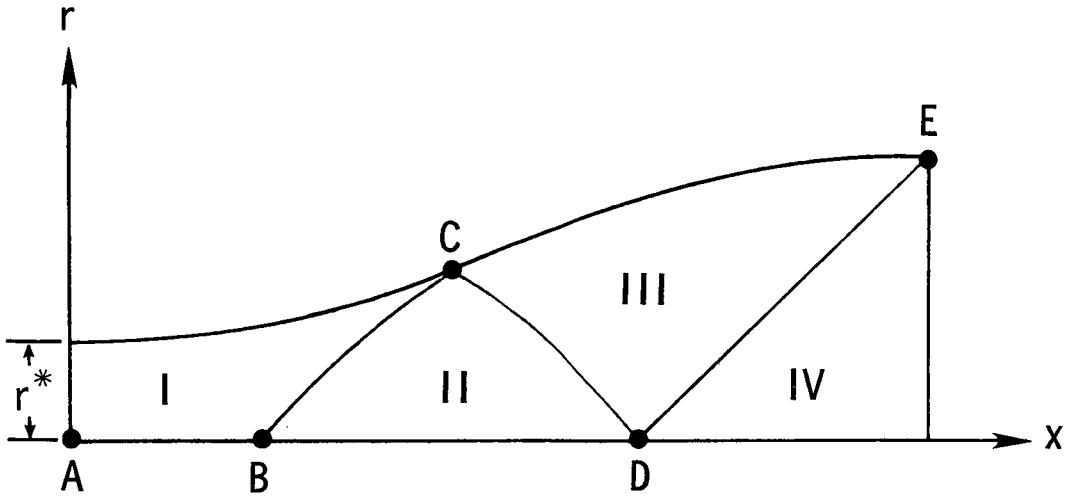

(a) Design method of characteristics.

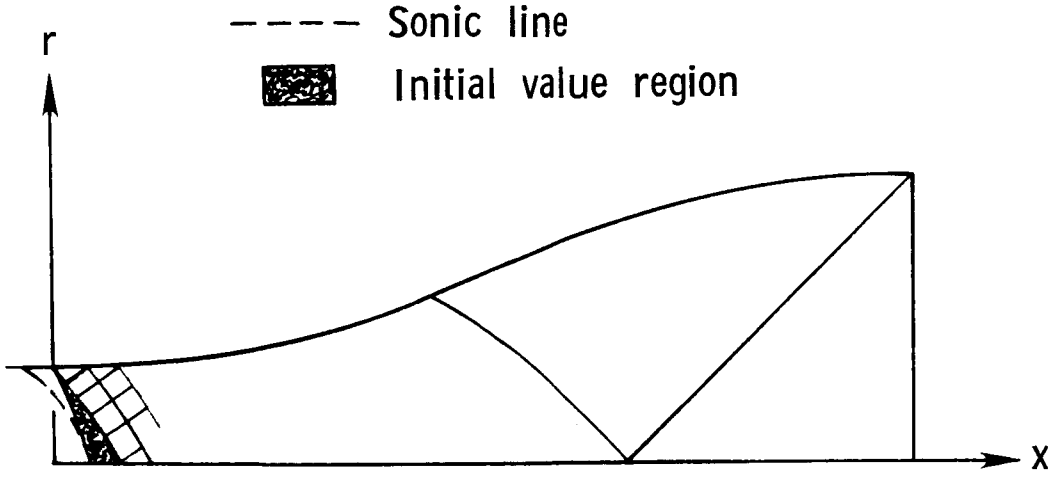

(b) Analysis method of characteristics.

Figure 1. Diagram of supersonic wind-tunnel nozzle.

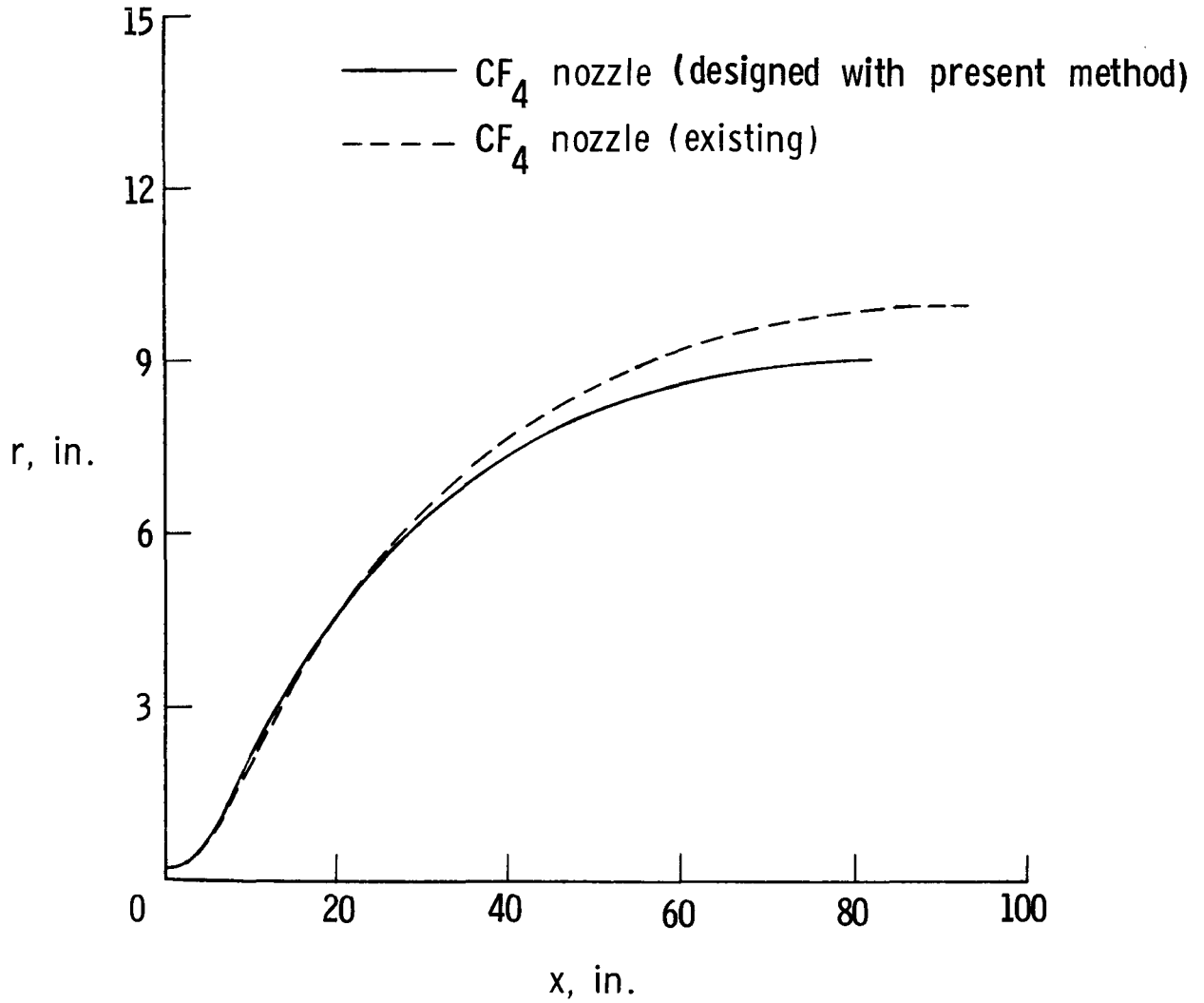

Figure 2. Comparison of existing and corrected CF_4 nozzle contours. $M_2 = 6$; $p_{t,1} = 2500$ psi; $T_{t,1} = 1260°R$.

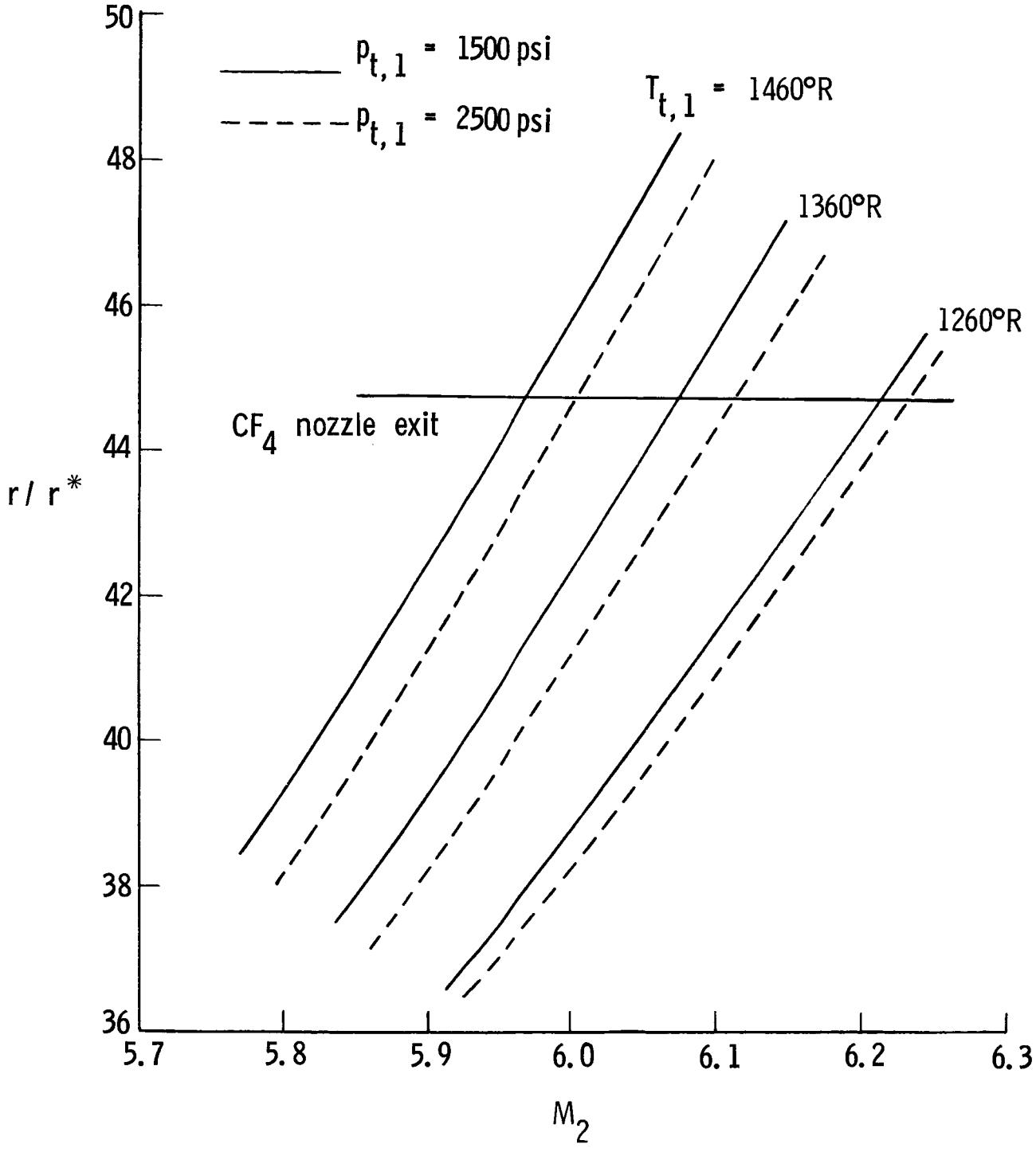

Figure 3. Exit radius as function of Mach number for one-dimensional inviscid flow of CF_4 gas.

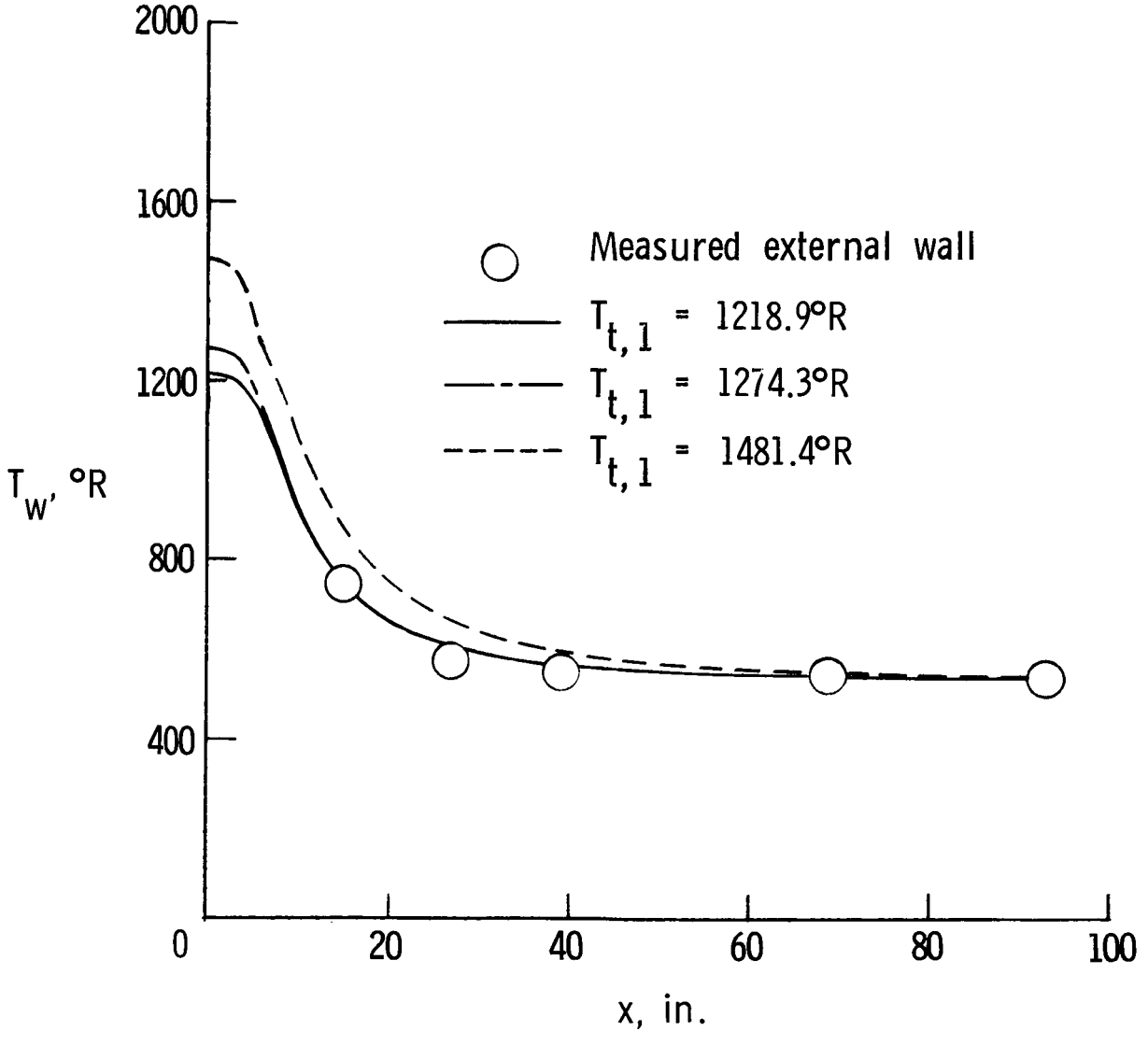

Figure 4. Theoretical and measured nozzle-wall temperature distributions.

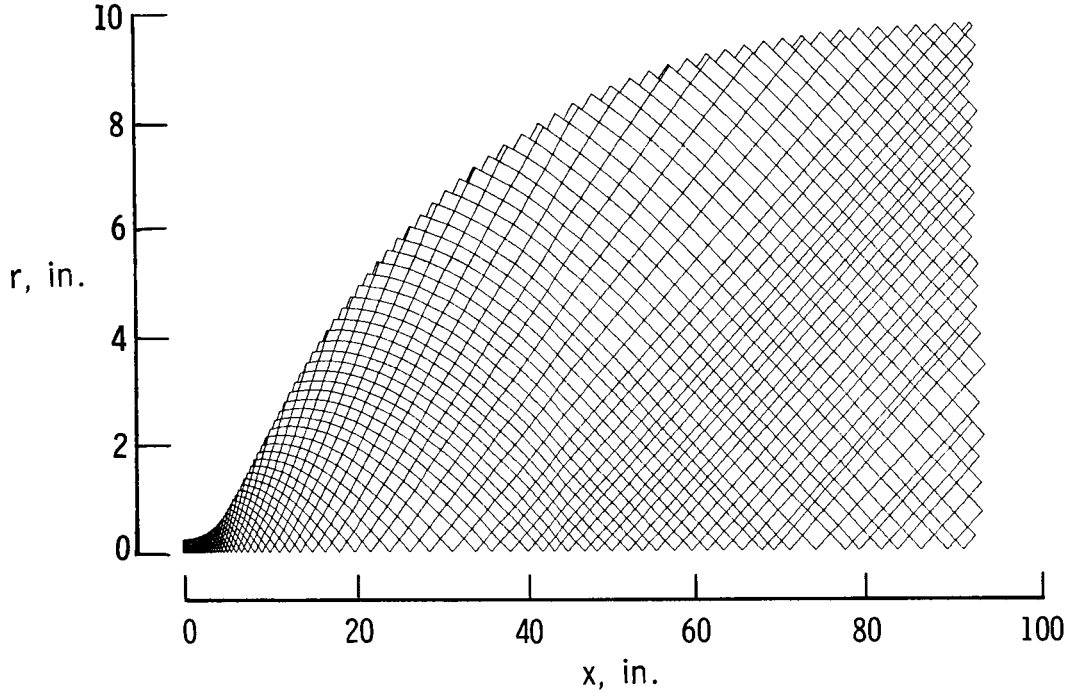

(a) Characteristic mesh.

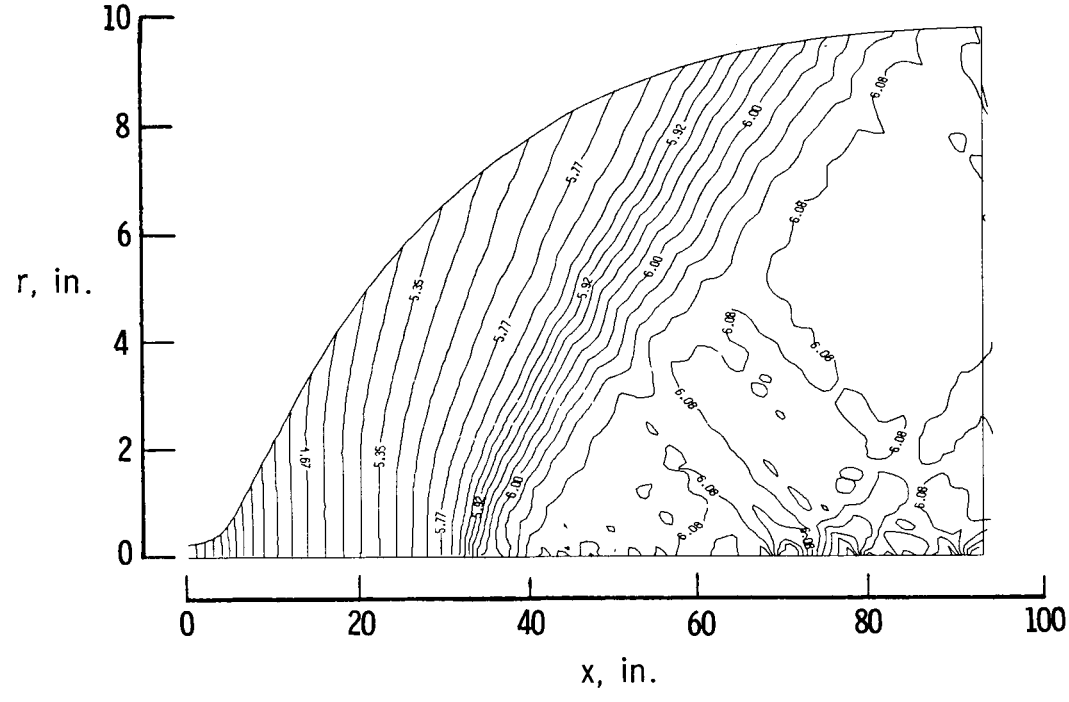

(b) Mach number contours.

Figure 5. Computational results for flow field in existing CF_4 nozzle. $p_{t,1} = 1742$ psi; $T_{t,1} = 1274.3°$R.

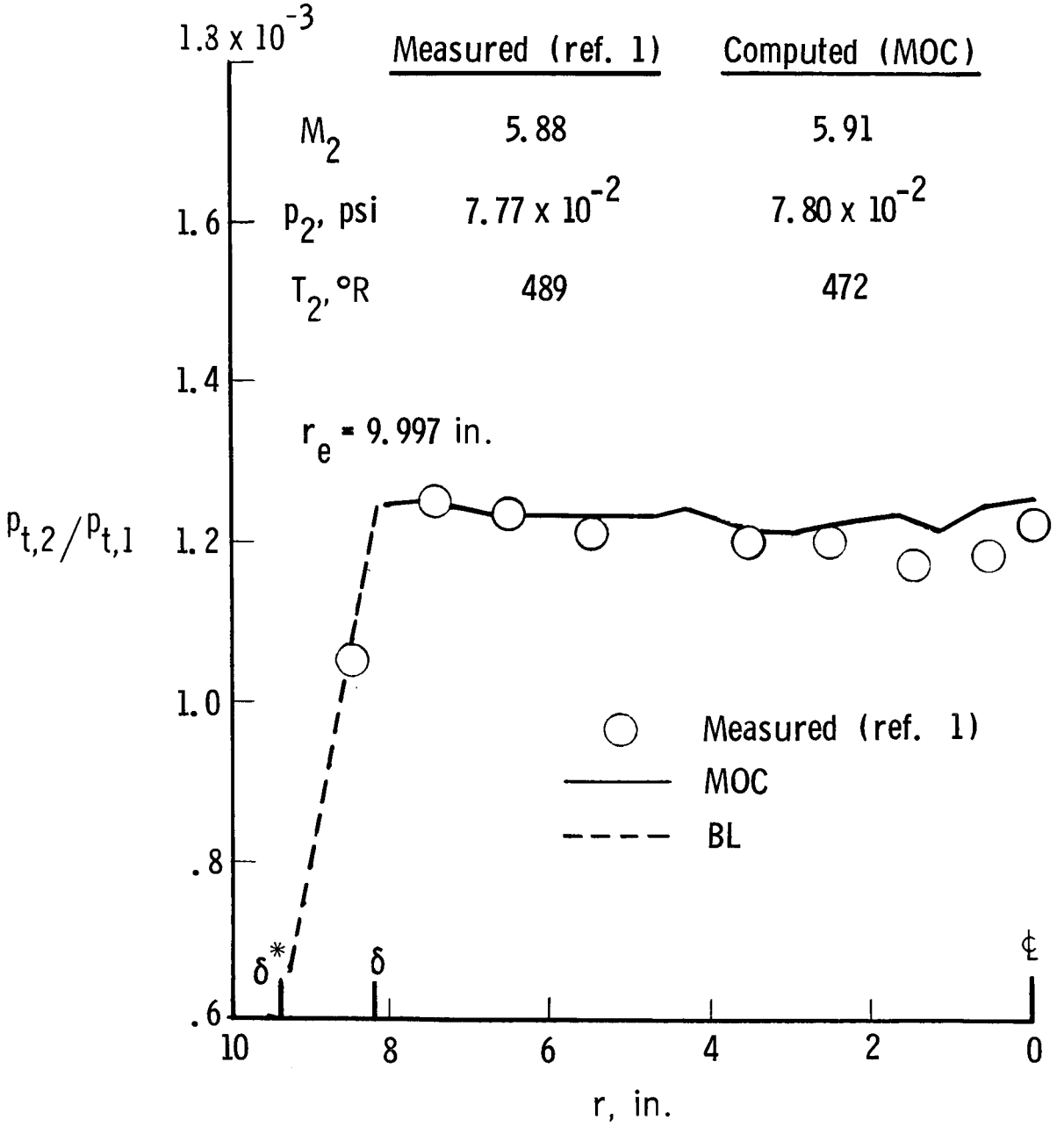

(a) $p_{t,1} = 2552$ psi; $T_{t,1} = 1481.4°$R.

Figure 6. Comparison of computed and measured pitot pressure profiles across test section at nozzle exit.

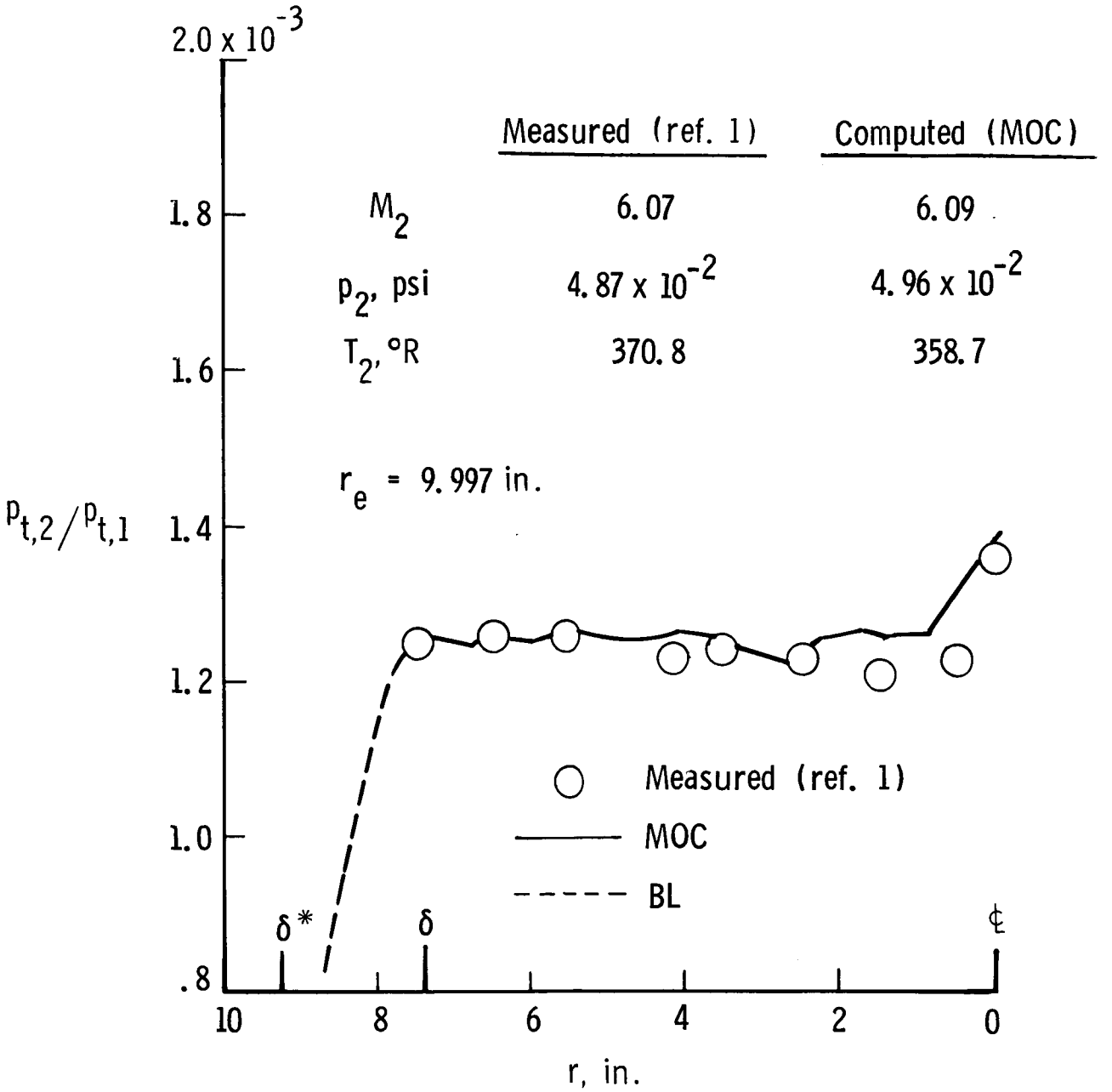

(b) $p_{t,1} = 1742$ psi; $T_{t,1} = 1274.3°$R.

Figure 6. Continued.

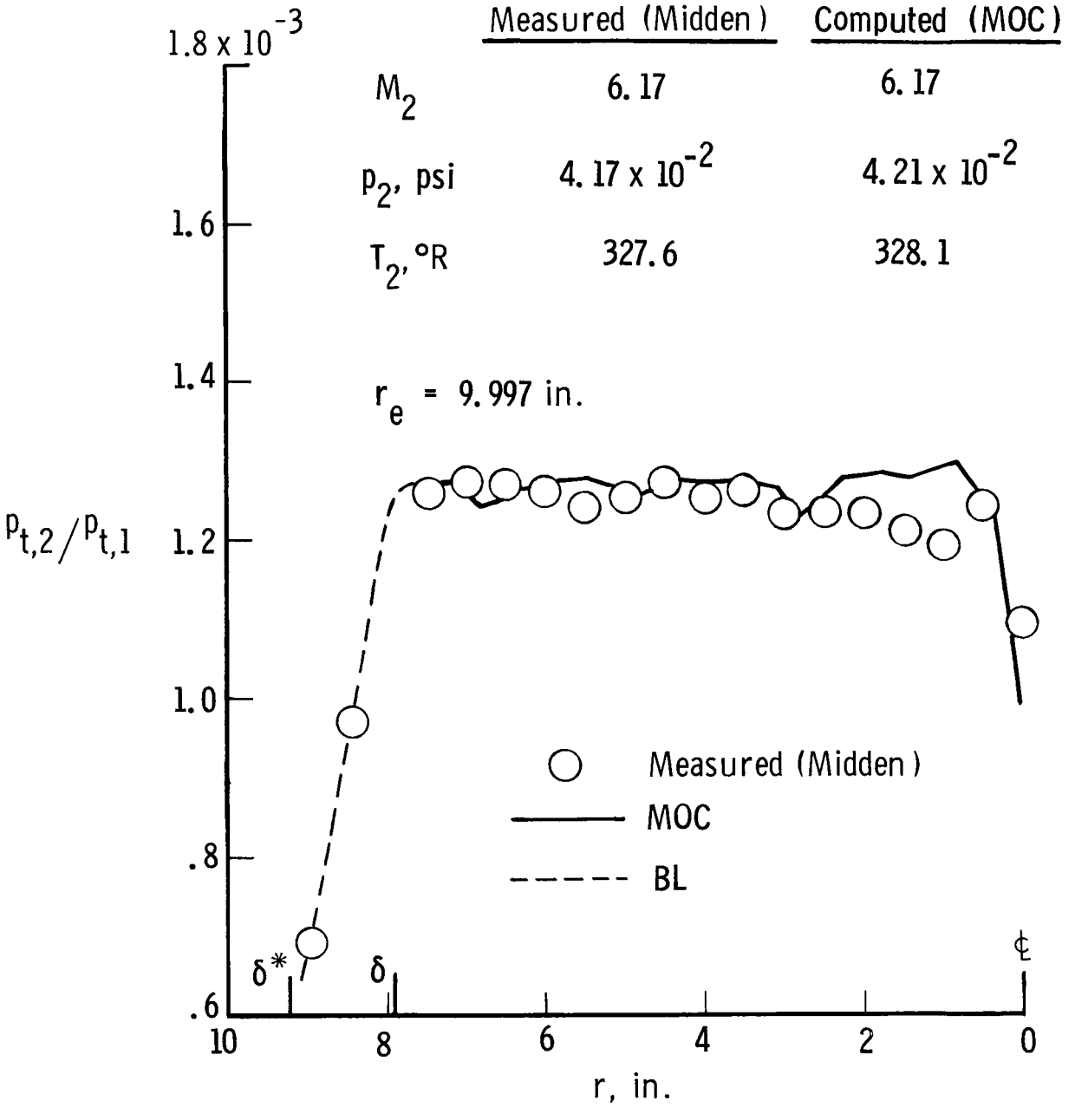

(c) $p_{t,1} = 1515$ psi; $T_{t,1} = 1218.9°$R.

Figure 6. Concluded.

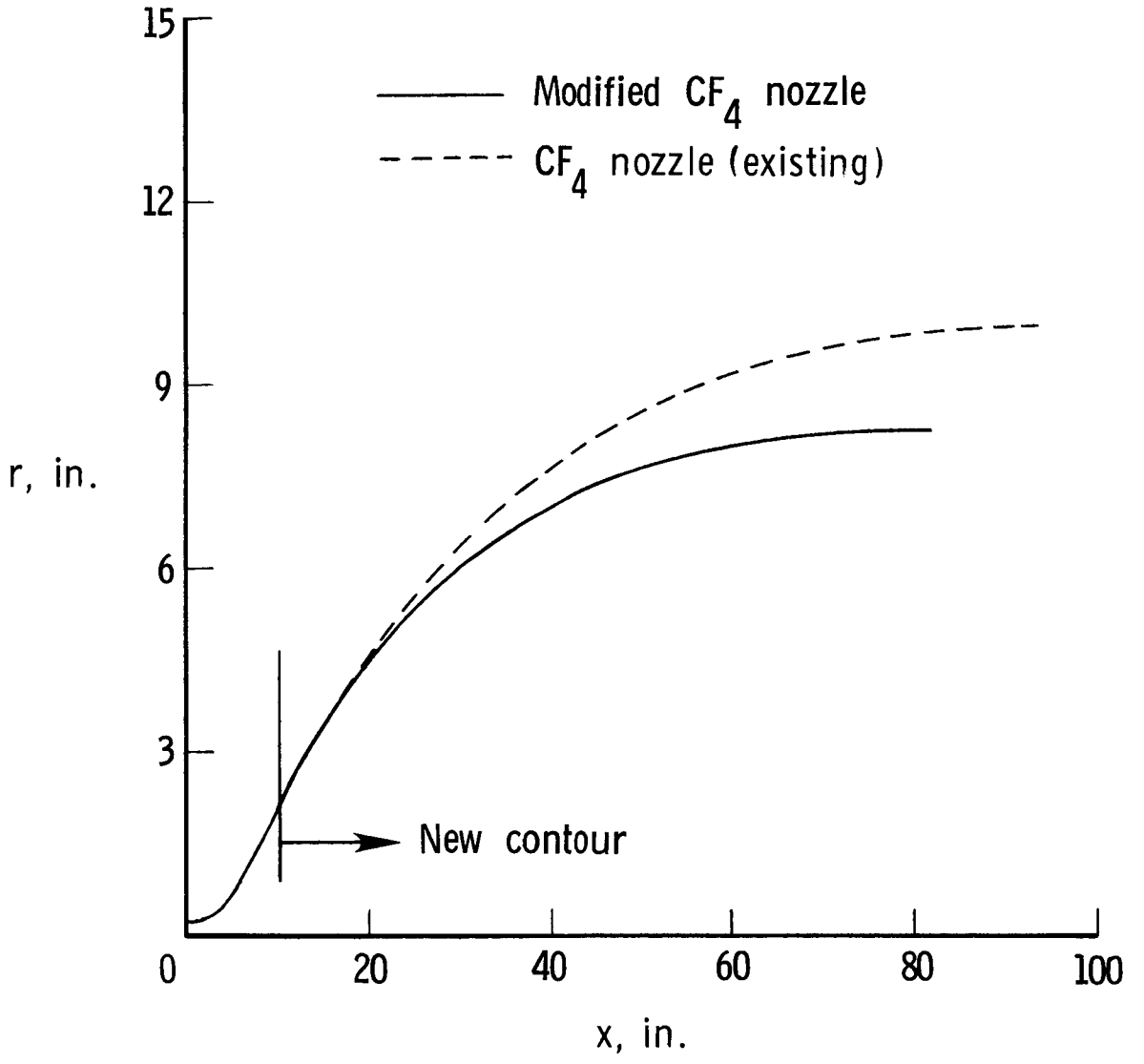

Figure 7. Modified CF_4 nozzle contour for $p_{t,1} = 1500$ psi, $T_{t,1} = 1260°R$, and $M_2 = 6$.

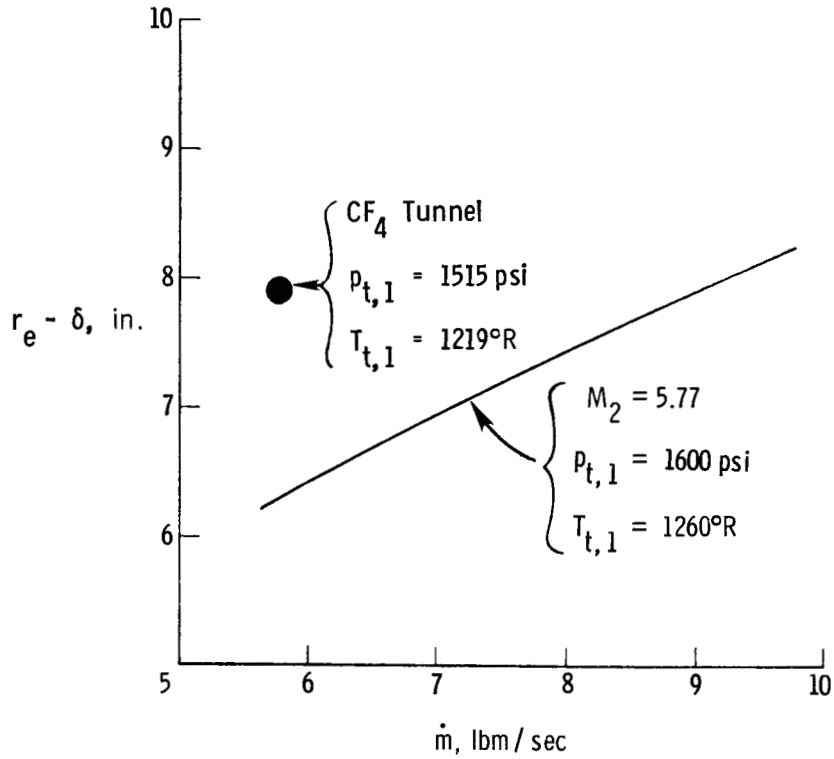

Figure 8. Inviscid CF_4 nozzle-exit radius as function of one-dimensional mass flow rate.

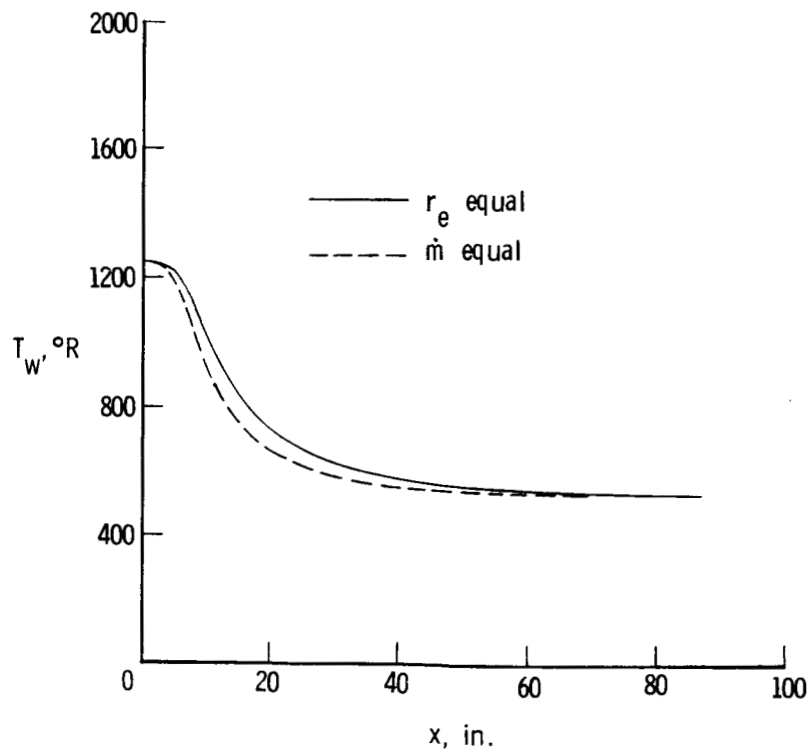

Figure 9. Theoretical wall temperature distributions for new CF_4 nozzles. $T_{t,1} = 1260°R$.

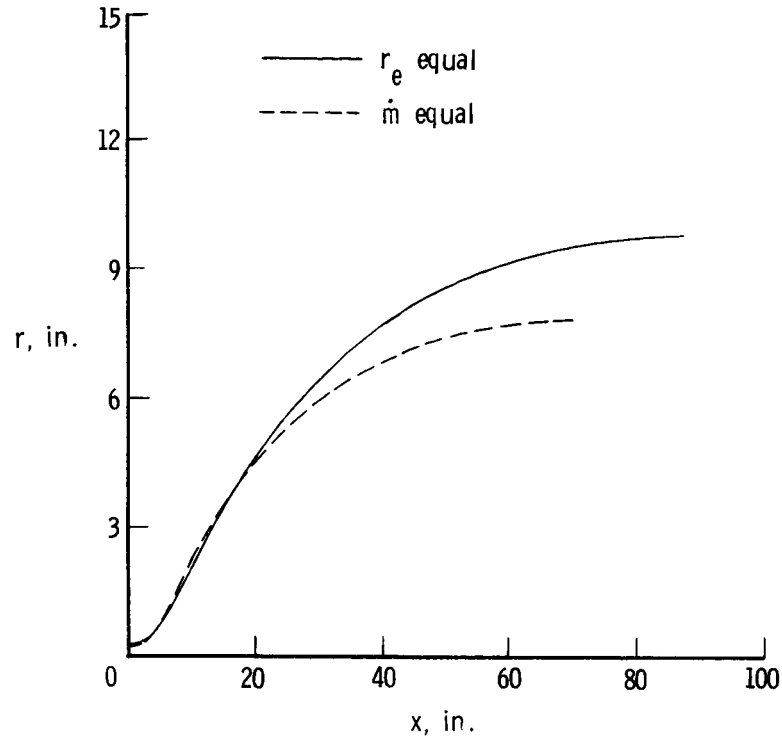

Figure 10. New CF_4 nozzle contours. $M_2 = 5.77$; $p_{t,1} = 1600$ psi; $T_{t,1} = 1260°R$.

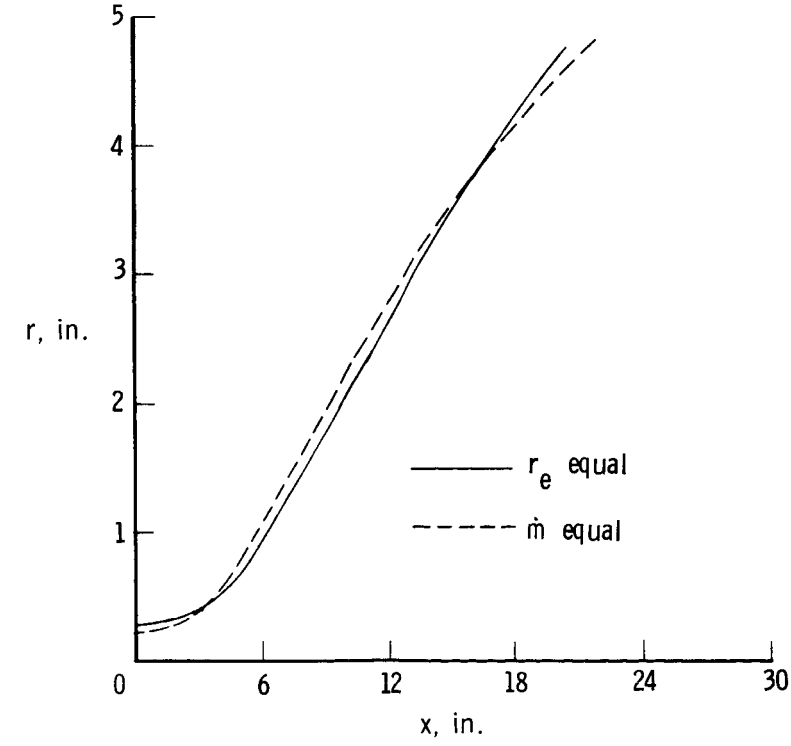

Figure 11. New CF_4 nozzle contours in throat region. $M_2 = 5.77$; $p_{t,1} = 1600$ psi; $T_{t,1} = 1260°R$.

Standard Bibliographic Page

1. Report No.	2. Government Accession No.	3. Recipient's Catalog No.
NASA TM-89042		

4. Title and Subtitle	5. Report Date
Computational Analysis and Preliminary Redesign of the Nozzle Contour of the Langley Hypersonic CF_4 Tunnel	March 1987
	6. Performing Organization Code: 506-40-11-02
7. Author(s): R. A. Thompson and Kenneth Sutton	8. Performing Organization Report No.: L-16170
9. Performing Organization Name and Address: NASA Langley Research Center, Hampton, VA 23665-5225	10. Work Unit No.
	11. Contract or Grant No.
12. Sponsoring Agency Name and Address: National Aeronautics and Space Administration, Washington, DC 20546-0001	13. Type of Report and Period Covered: Technical Memorandum
	14. Sponsoring Agency Code

15. Supplementary Notes

16. Abstract

A computational analysis, modification, and preliminary redesign study was performed on the nozzle contour of the Langley Hypersonic CF_4 Tunnel. This study showed that the existing nozzle was contoured incorrectly for the design operating condition, and this error was shown to produce the measured disturbances in the exit flow field. A modified contour was designed for the current nozzle downstream of the maximum turning point that would provide a uniform exit flow. New nozzle contours were also designed for an exit Mach number and Reynolds number combination which matches that attainable in the Langley 20-Inch Mach 6 Tunnel. Two nozzle contours were designed: one having the same exit radius but a larger mass flow rate than that of the existing CF_4 Tunnel, and the other having the same mass flow rate but a smaller exit radius than that of the existing CF_4 Tunnel.

17. Key Words (Suggested by Authors(s))	18. Distribution Statement
Wind-tunnel nozzle Hypersonic Method of characteristics CF_4 gas	Unclassified—Unlimited Subject Category 09

19. Security Classif.(of this report)	20. Security Classif.(of this page)	21. No. of Pages	22. Price
Unclassified	Unclassified	30	A03

For sale by the National Technical Information Service, Springfield, Virginia 22161

NASA-Langley, 1987